

# Inactivation and Inhibition of $\gamma$ -Aminobutyric Acid Aminotransferase by Conformationally Restricted Vigabatrin Analogues

Sun Choi<sup>†</sup> and Richard B. Silverman\*

Department of Chemistry, Department of Biochemistry, Molecular Biology, and Cell Biology, and the Drug Discovery Program, Northwestern University, Evanston, Illinois 60208-3113

Received March 25, 2002

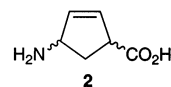
Four cyclohexene analogues of  $\gamma$ -aminobutyric acid (GABA) and  $\beta$ -alanine were designed as conformationally rigid analogues of the epilepsy and drug addiction drug vigabatrin and as potential mechanism-based inactivators of  $\gamma$ -aminobutyric acid aminotransferase (GABA-AT). The corresponding cyclopentene analogues were previously reported to be inhibitors, but not inactivators, of GABA-AT (Qiu, J.; Pingsterhaus, J.; Silverman, R. B. *J. Med. Chem.* **1999**, *42*, 4725–4728). *cis*-3-Aminocyclohex-4-ene-1-carboxylic acid (**3**) and *cis*-2-aminocyclohex-3-ene-1-carboxylic acid (**5**) showed time- and concentration-dependent, irreversible inactivation of GABA-AT. In both cases, the inactivations are protected by substrate, indicating that they are active site-directed. *trans*-3-Aminocyclohex-4-ene-1-carboxylic acid (**4**) and *trans*-2-aminocyclohex-3-ene-1-carboxylic acid (**6**) are not inactivators but are competitive reversible inhibitors of GABA-AT. Unlike the cyclopentene analogues, there appears to be sufficient ring flexibility to allow inactivation to occur. The orientation of the carboxylic and amino groups of these analogues is important for their binding to GABA-AT. Molecular modeling of GABA-AT with **3–6** and molecular dynamics simulations with vigabatrin bound provide rationalizations for the inhibitory properties of these compounds.

## Introduction

$\gamma$ -Aminobutyric acid (GABA) is an important inhibitory neurotransmitter in the mammalian central nervous system.<sup>1</sup> The major pathway for its degradation is via transamination with  $\alpha$ -ketoglutarate catalyzed by the pyridoxal 5'-phosphate (PLP)-dependent enzyme GABA aminotransferase (GABA-AT, E. C. 2.6.1.19).<sup>2</sup> Inhibition of this enzyme results in an increase in availability of GABA, which can have a beneficial effect on neurological disorders including epilepsy,<sup>3</sup> Parkinson's disease,<sup>4</sup> Huntington's chorea,<sup>4b,5</sup> and Alzheimer's disease.<sup>6</sup> Recently, it has been found that an increase in GABA also blocks the effects of drug addiction.<sup>7</sup>

Selective inactivation of GABA-AT by 4-aminohept-5-enoic acid (**1**, Scheme 1;  $\gamma$ -vinyl-GABA or vigabatrin),<sup>8,9</sup> a mechanism-based inactivator<sup>10</sup> of the enzyme, is already being successfully applied in the treatment of epilepsy<sup>11</sup> and is in clinical trials for the treatment of drug addiction.<sup>12</sup> A detailed study of the mechanism of inactivation of GABA-AT by vigabatrin revealed that it acted by two principal inactivation pathways: a Michael addition mechanism (pathway a), which accounts for about 70% of the total inactivation, and an enamine mechanism (pathway b, Scheme 1), which accounts for about 30% of the inactivation.<sup>13</sup> These two pathways occur via deprotonation of the  $\gamma$ -carbon followed by tautomerization through either the PLP ring (pathway a, leading to a Michael addition) or the vinyl double bond (pathway b, leading to an enamine formation).

Presumably, the reason that two inactivation mechanisms arise is because the orientations of the pyridoxal ring system and the vinyl  $\pi$ -orbitals relative to the electrons in the  $\gamma$ -C–H bond of  $\gamma$ -vinyl-GABA allow delocalization of those electrons in either direction.<sup>13</sup> A molecular model of vigabatrin bound to the PLP supported the possibility that the lysine residue that removes the  $\gamma$ -proton (B in Scheme 1) could then become the acid donor (B<sup>+</sup>–H in Scheme 1) for either the cofactor (pathway a) or the vinyl group (pathway b).<sup>14</sup>

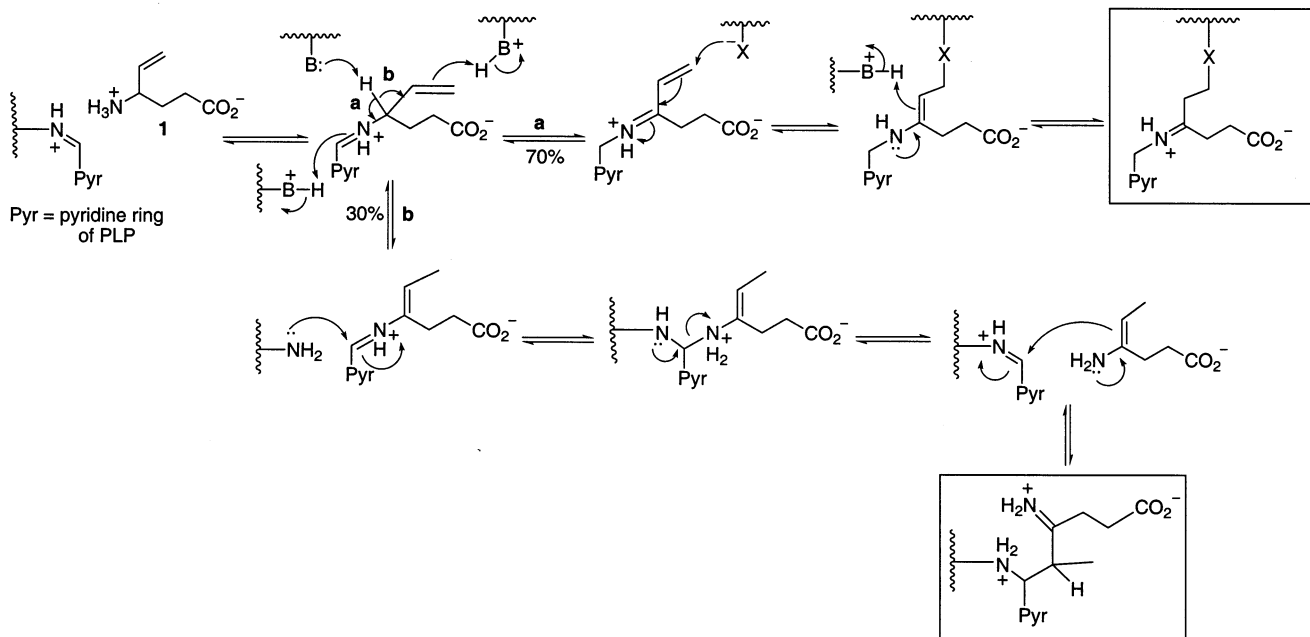


We wanted to design an inactivator that functioned only through one inactivation mechanism and thought that by constraining the vinyl  $\pi$ -orbitals in a conformationally rigid analogue of vigabatrin, such as 4-amino-2-cyclohexene-1-carboxylic acid (**2**), one of the two inactivation pathways may be excluded.<sup>15</sup> Unfortunately, **2** is so constrained that neither the *cis* nor the *trans* analogue is an inactivator of GABA-AT, although the *cis* isomer is an excellent substrate and the *trans* isomer is a competitive inhibitor. A molecular model of vigabatrin bound in GABA-AT indicated that prevention of rotation of the vigabatrin vinyl group should prevent the Michael addition pathway,<sup>14</sup> so a slightly less conformational constraint was needed. To provide more flexibility for the double bond, the corresponding cyclohexene vigabatrin analogues (**3–6**) were designed and synthesized. Compound **3** was found to be a time-dependent inactivator, which did indeed inactivate GABA-AT by only one mechanism (analogous to path-

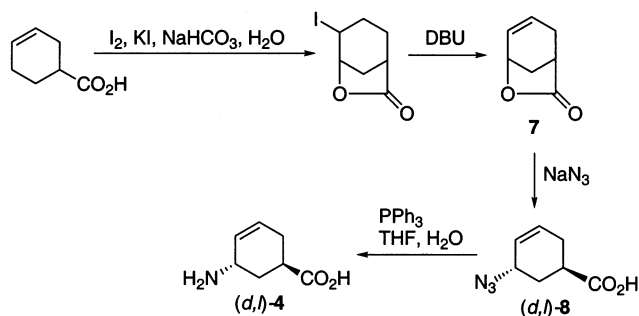
\* To whom correspondence should be addressed. Tel: (847)491-5653. Fax: (847)491-7713. E-mail: Agman@chem.northwestern.edu.

<sup>†</sup> Current address: Tripos, Inc. 1699 South Hanley Road, St. Louis, MO 63144.

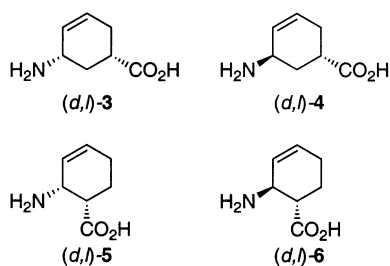
Scheme 1



Scheme 2



way b in Scheme 1).<sup>14</sup> Here, we report the inactivation of GABA-AT by **5**, the reversible inhibition by **4** and **6**, and rationalize their activity by molecular modeling.

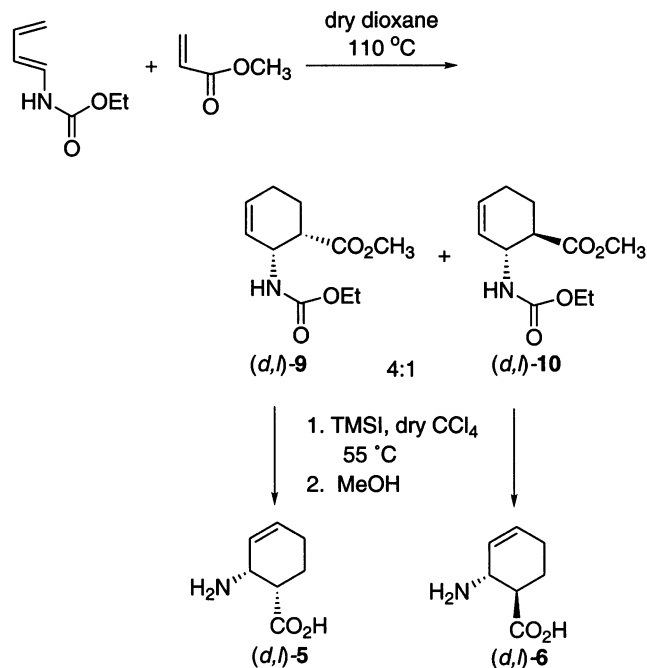


## Chemistry

The preparation of (*d,l*)-*trans*-3-azidocyclohex-4-ene-1-carboxylic acid (**8**) was carried out by  $S_N2$  azide substitution<sup>16</sup> of 7-oxabicyclo[3,2,1]oct-2-en-6-one (**7**), which was synthesized from cyclohex-3-ene-1-carboxylic acid by the procedure of Marshall et al. (Scheme 2).<sup>17</sup> Subsequent reduction of the allyl azide with  $PPh_3$  in tetrahydrofuran (THF) with 1 equiv of water<sup>18</sup> gave (*d,l*)-**4**.

A mixture of ethyl *cis*- and *trans*-6-carbomethoxy-2-cyclohexen-1-yl carbamates (**9** and **10**, in a 4:1 ratio) was prepared from the Diels–Alder reaction of ethyl *trans*-1,3-butadiene-1-carbamate and methyl acrylate,<sup>19</sup> which

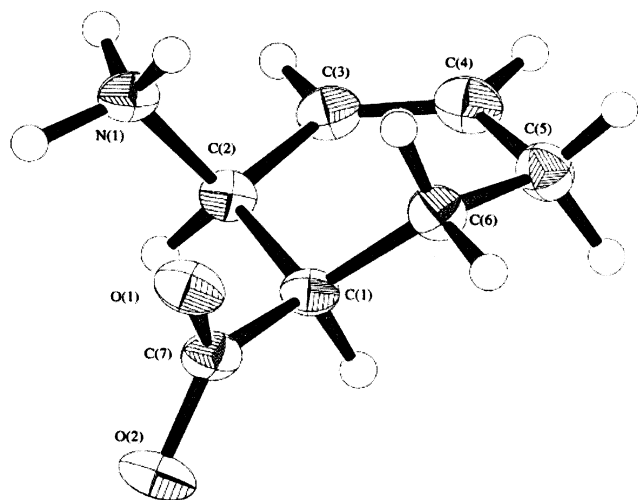
Scheme 3



were separated by repeated silica gel column chromatography (Scheme 3). The alkyl carbamate and alkyl ester groups in each isomer were deprotected simultaneously with iodotrimethylsilane,<sup>20</sup> and **5** and **6** were purified by ion exchange chromatography. The structure of **5** was confirmed by X-ray crystallography (Figure 1).

## Results and Discussion

Incubation of GABA-AT with **3**<sup>14</sup> and **5** led to time- and concentration-dependent inactivation of the enzyme. A Kitz and Wilson replot<sup>21</sup> of the data gave the kinetic constants shown in Table 1. After they were gel-filtered, no return of enzyme activity was observed, supporting the irreversible nature of the inactivation. In the presence of GABA, the rate of inactivation

**Figure 1.** ORTEP drawing of **5**.**Table 1.** Kinetic Constants for the Cyclohexene Analogues<sup>a</sup>

compd	$k_{\text{inact}}$ ( $\text{min}^{-1}$ )	$K_{\text{I}}$ (mM)	$k_{\text{inact}}/K_{\text{I}}$ ( $\text{min}^{-1} \text{mM}^{-1}$ )	$K_{\text{I}}$ ( $\mu\text{M}$ )
<b>3</b> <sup>a</sup>	0.01	2.3	0.0042	
<b>4</b>				100
<b>5</b>	0.03	13.0	0.0024	
<b>6</b>				125
vigabatrin	0.24	0.85	0.28	

<sup>a</sup> Choi, S.; Storici, P.; Schirmer, T.; Silverman, R. B. *J. Am. Chem. Soc.* **2002**, *124*, 1620–1624.

diminished, indicating that the reaction occurs at the active site of the enzyme. The trans isomers, **4** and **6**, however, showed no time-dependent inhibition of the enzyme, but they were potent competitive reversible inhibitors (Table 1).

Inactivation by **3**<sup>14</sup> and **5** is quite remarkable, given that the corresponding cyclopentene analogue **2** does not inactivate the enzyme.<sup>15</sup> By analogy to the two mechanisms of inactivation of GABA-AT by vigabatrin (Scheme 1),<sup>13</sup> **5** could react by one or both of these possible mechanisms (Scheme 4). Expansion of the cyclopentene ring by one methylene provides sufficient conformational flexibility to allow for tautomerization and rearrangement of the enamine (pathway b) but presumably not for nucleophilic attack (pathway a). Recently, we found that **3** inactivates GABA-AT exclusively by the enamine mechanism.<sup>14</sup> This was rationalized based on molecular modeling results, using coordinates from the X-ray crystal structure of pig liver GABA-AT,<sup>22</sup> which show that the lysine residue that binds to the PLP cofactor, known to be the residue labeled by vigabatrin,<sup>23</sup> is not aligned with the vinyl group in its lowest energy orientation (Figure 2A); rotation of the vinyl group is imperative for nucleophilic attack by that lysine residue (Figure 2B). Consequently, both tautomerization and inactivation pathways could occur.

To gain further evidence to support the requirement for vinyl group rotation, a molecular dynamics (MD) simulation of the vigabatrin–enzyme complex was carried out by raising the temperature to 500 K over a period of 5000 fs to excite all of the bonds in the protein randomly, followed by cooling to 300 K over a period of 5000 fs to allow the bonds in the complex to reach equilibrium (Figure 3A). The distances between the side

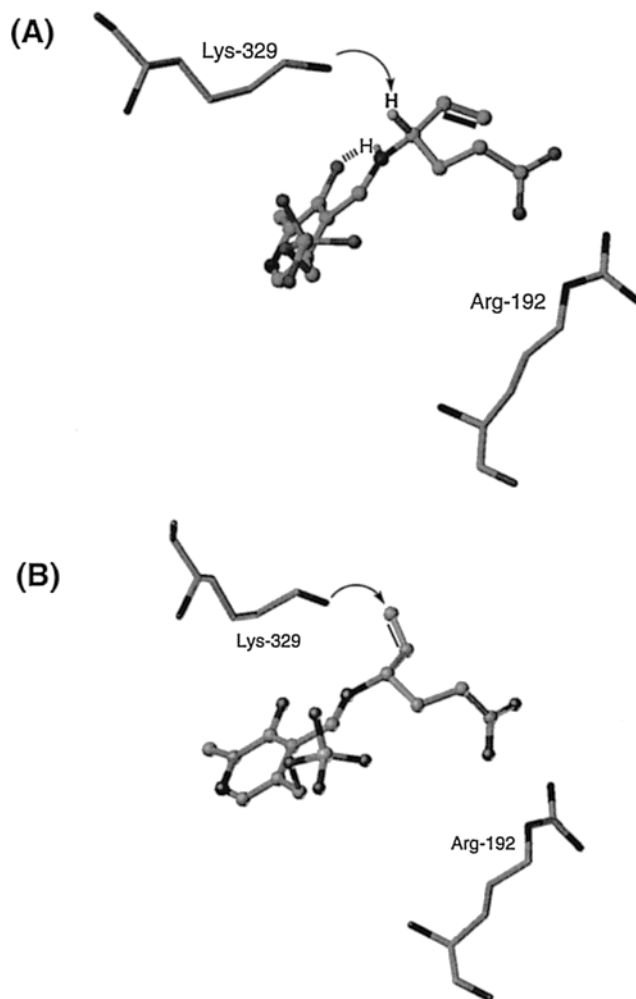
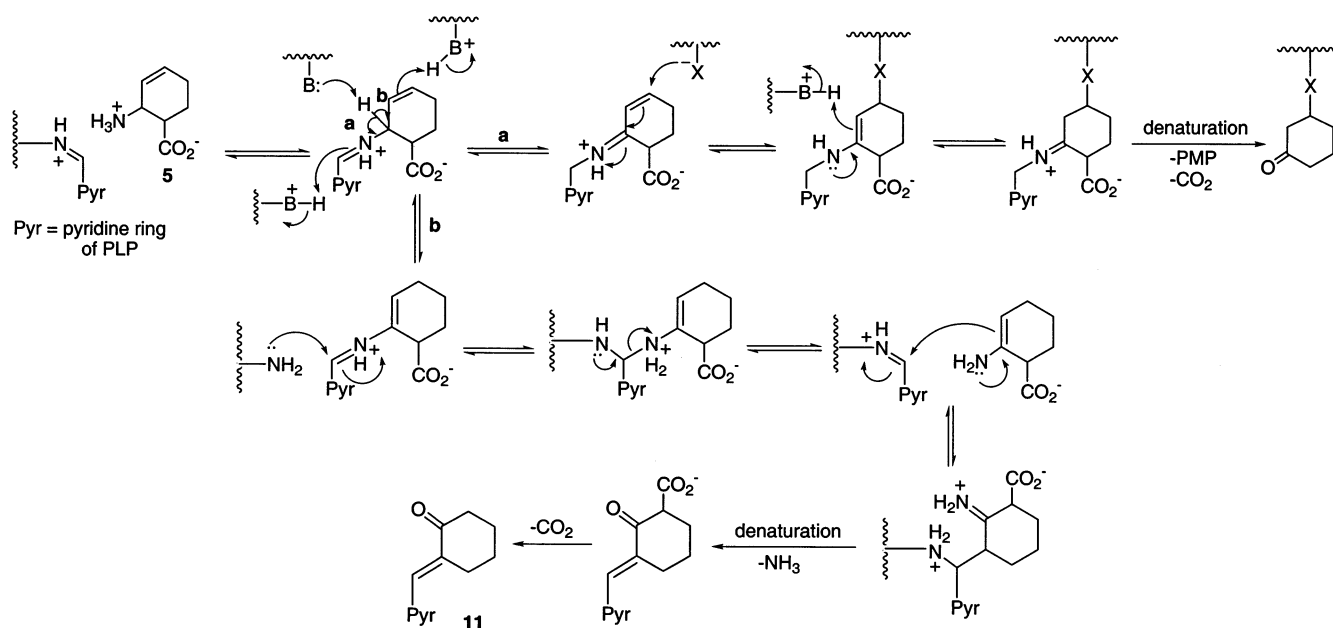


**Figure 2.** (A) Molecular modeling of vigabatrin bound to show that Lys-329 is not in the correct orientation for Michael addition. Only the  $\gamma$ -H and Schiff base N–H are explicitly displayed; the rest of the hydrogens are omitted for clarity. (B) Molecular model to show that Michael addition requires the vinyl group to rotate toward Lys-329.

chain nitrogen of Lys-329 and the terminal carbon of the vinyl group were examined from the recorded trajectories of the simulation. After it reached equilibrium, the distances were mostly in the range of 3.2–4.1 Å (Figure 3B), indicating that the rotatable vinyl group would be close enough to the nucleophilic amino group in the flexible side chain of Lys-329 to allow for Michael addition (Figure 2). In the case of **3**, the conformational rigidity of the cyclohexene ring prohibits the double bond from rotating sufficiently to allow nucleophilic addition (data not shown), which results in only pathway b as the inactivation pathway.<sup>14</sup>

Compound **5**, however, can bind in two important conformations, which could allow for tautomerization by both pathways and multiple inactivation products. Figure 4 shows both conformers from two different perspectives; conformer A does not allow Michael addition after tautomerization, but B does allow Michael addition. The observation of pyridoxamine 5'-phosphate (PMP) after denaturation of the inactivated enzyme signals the Michael addition mechanism (see Scheme 4, pathway a), and the observation of modified cofactor with a  $T_{\text{R}}$  in the range of 34–35 min in our high-performance liquid chromatography (HPLC) system

Scheme 4



denotes the enamine mechanism (Scheme 4, pathway b). In fact, inactivation of GABA-AT reconstituted with [ $^3\text{H}$ ]PLP by **5** followed by HPLC separation of the coenzyme-derived products gave tritiated PLP, PMP, and multiple products in the region where modified coenzyme adducts occur ( $T_R = 35$  min) (Figure 5), whereas **3** gave only a single peak (at  $T_R = 34$  min).<sup>14</sup> It is not clear if the multiple products at the longer retention times contain decomposition products of the enamine pathway adduct or possibly carboxylated and decarboxylated forms. The proposed modified cofactor (**11**, Scheme 4) was synthesized by aldol condensation of PLP with cyclohexanone and was shown to have the same HPLC retention time and mass as the expected product obtained by enzyme inactivation.

The inability of the trans isomers to inactivate GABA-AT appears to be related to their binding orientations at the active site. A homology modeling-deduced active site structure of GABA-AT was previously reported,<sup>24</sup> which was used to explain the substrate specificity and stereospecificity of the enzyme, as well as the unique reactivity of the *S* isomer as compared to the *R* isomer of vigabatrin as a mechanism-based inactivator. Only the reactive *S* isomer of vigabatrin has the scissile  $\gamma\text{-C-H}$  bond perpendicular to the coenzyme ring plane and the  $\gamma$ -proton readily accessible to Lys-329, the proposed general base of the reaction. The inactive *R* isomer has the vinyl group directed toward Lys-329 and the  $\gamma\text{-C-H}$  bond toward Arg-445, making the  $\gamma$ -proton inaccessible to Lys-329.<sup>24</sup> This same phenomenon was demonstrated in modeling studies with the X-ray crystal structure of pig liver GABA-AT,<sup>22</sup> whose active site residues, which are within a distance of 10 Å from the cofactor, have identical counterparts with human brain GABA-AT. It is probable that the active species in racemic cis inactivator **3** has the *S* configuration as in the case of vigabatrin, but because of the movement of the carboxylate group in **5** to the carbon adjacent to the amino group, the same stereochemistry in **5** is called the *R* configuration to accommodate the *R/S* nomenclature rules. These compounds probably are involved in

the same electrostatic interactions of their carboxylate group with the active site Arg-192 for binding, as shown by modeling of vigabatrin or GABA.<sup>22,24</sup> Our docking studies also confirmed this. Another interesting result observed from the docking of these regioisomers is their internal hydrogen-bonding interactions. The *S* isomer of inactivator **3** exhibits the normal internal hydrogen-bonding pattern (i.e., between the aldimine N-H and the hydroxyl O of PLP) (Figure 6A). However, the internal hydrogen-bonding partner of the N-H in the aldimine of inactivator **5** with the same stereochemistry is switched to the carboxylate (Figure 6B). This H-bond interchange appears to optimize the conformation of the aldimine of **5** to maintain the binding interaction between the carboxylate and the Arg-192 and at the same time to orient the  $\gamma\text{-H}$  properly for reactivity with Lys-329.

On the other hand, the *R* enantiomer of the trans inhibitor **4** and the *S* enantiomer of **6** (which has the same stereochemistry as the *R* enantiomer of **4**) should be the actual competitive inhibition species to accommodate their binding at the active site with the same electrostatic interactions of their carboxylate group with Arg-192 (Figure 7). When this salt bridge forms, however, the proton that must be abstracted in order for inactivation to occur (the equivalent to the  $\gamma$ -proton in GABA) is oriented away from Lys-329, preventing its removal. Therefore, it competitively binds, but catalysis cannot be initiated, so inactivation does not occur.

For comparison, the *cis*-cyclopentene vigabatrin analogue (1*R*,4*S*)-(+)-**2**, which showed good substrate activity (actually better than GABA),<sup>15</sup> was docked into the enzyme (Figure 8A). It also binds well at the active site, directed by the salt bridge interaction between the carboxylate and the Arg-192. After it binds, its  $\gamma\text{-H}$  is positioned properly for abstraction by the active site base, Lys-329 (at a distance of 2.7 Å). Furthermore, this proton is oriented perpendicular to the plane of the pyridine ring (with a torsional angle C=N-C-H of about 82°), making the  $\gamma\text{-H-C}$  bond easily broken according to the Dunathan Postulate, i.e., the orienta-



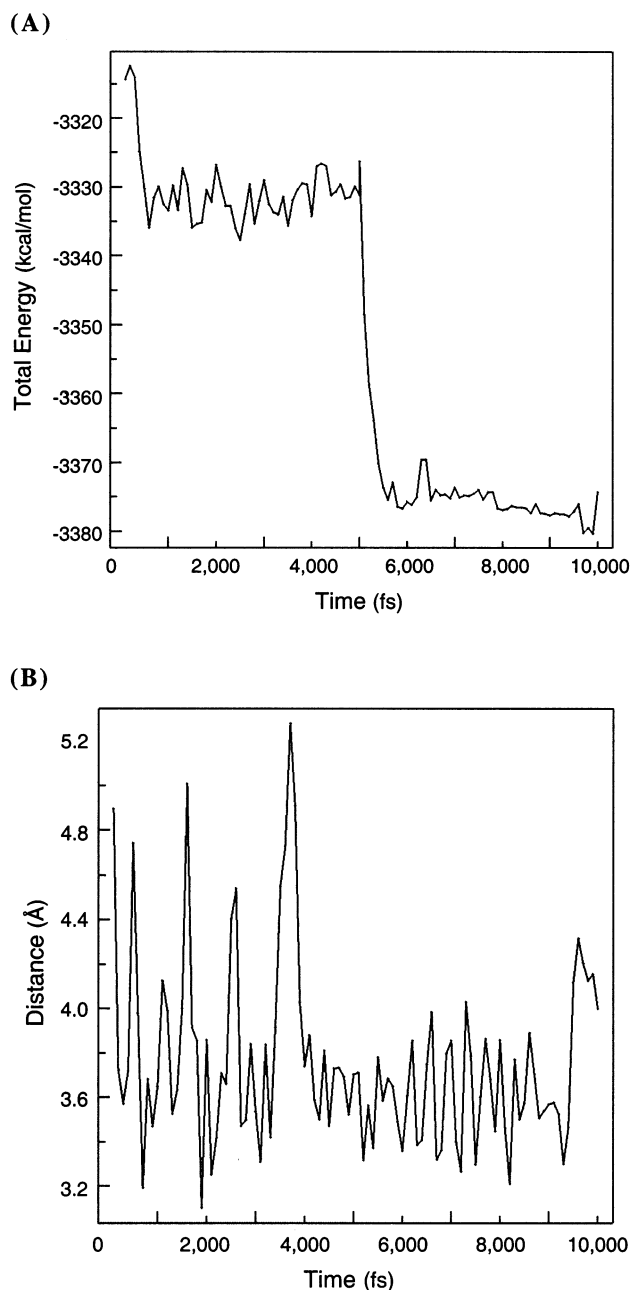


**Figure 3.** (A) Total energy of the vigabatrin–enzyme complex during MD simulation by raising the temperature to 500 K over a period of 5000 fs and cooling to 300 K over a period of 5000 fs. (B) Snapshot distances between the side chain nitrogen of Lys-329 and the terminal carbon of the vigabatrin vinyl group, measured at every 100 fs from the MD simulation.

tion of the bond to be cleaved should be perpendicular to the cofactor–substrate  $\pi$ -system.<sup>25</sup> This  $\gamma$ -C–H bond breakage, however, does not lead to mechanism-based inactivation of the enzyme because there is neither a nucleophile available for Michael addition nor a proton donor for the enamine mechanism. Instead, it is turned over as a substrate, presumably via the mechanism shown in Scheme 5. A comparison of a molecular model of **2** with GABA at the active site of the enzyme explains the stereospecificity of **2** (Figure 8B), namely, the same as that for GABA (the *pro-S* proton on C4 of GABA). Docking results show that the *pro-S* proton is properly oriented for abstraction by Lys-329 (at a distance of 2.2 Å) with a torsional angle of C=N–C–H of about 73°,

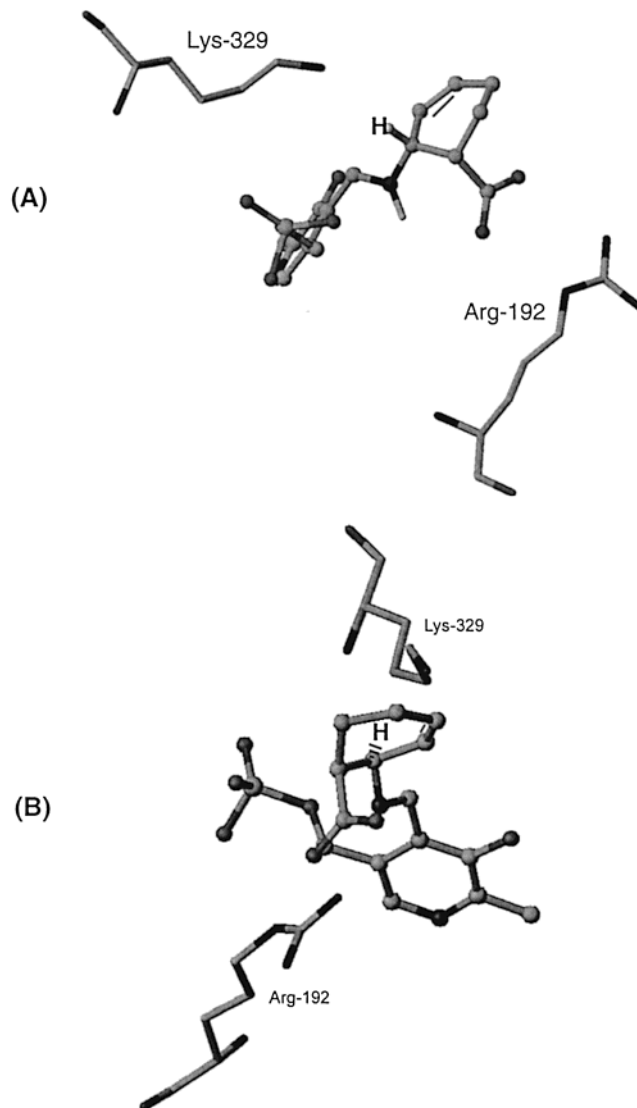


**Figure 4.** Molecular model of two low-energy conformations of **5**.

while maintaining the same electrostatic interaction of the carboxylate with the active site Arg-192 for binding.

In summary, these results demonstrate that the conformationally restricted, cyclohexene vigabatrin analogues **3** and **5** irreversibly inhibit GABA-AT, and inactivation occurs at the active site. Although **3** prohibits the Michael addition pathway, **5** allows both the Michael addition and the enamine pathways to operate. The corresponding trans isomers **4** and **6** are competitive reversible inhibitors of the enzyme because, once bound, the proton that needs to be removed for the reaction is not oriented toward the active site base (Lys-329). Therefore, the binding orientations of the carboxylic and amino groups are important to the type of inhibition that occurs, which suggests future structural modifications.

### Experimental Section

**General Methods.** <sup>1</sup>H and <sup>13</sup>C NMR spectra were recorded on Varian Gemini 300 MHz and Inova 500 MHz NMR spectrometers. Chemical shifts are reported as  $\delta$  values in parts per million (ppm) downfield from Me<sub>4</sub>Si ( $\delta$  0.0) as the internal standard in CDCl<sub>3</sub>. For samples run in D<sub>2</sub>O, the HOD resonance was arbitrarily set at 4.80 ppm. X-ray crystal

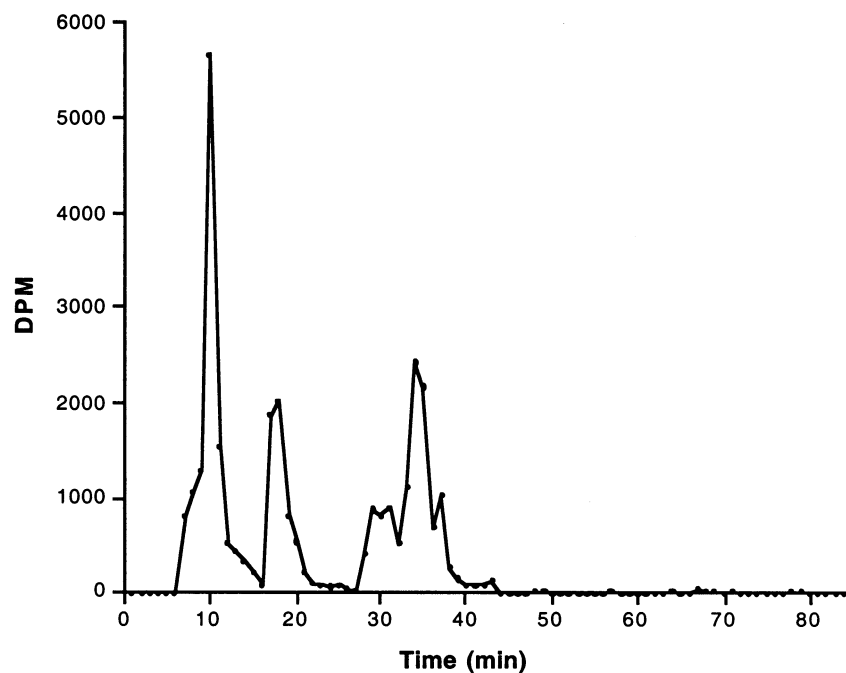


**Figure 5.** HPLC profile of **5** after inactivation of [ $^3\text{H}$ ]PLP-GABA-AT. The retention time of authentic PMP and PLP matched with the first and second peaks, respectively.

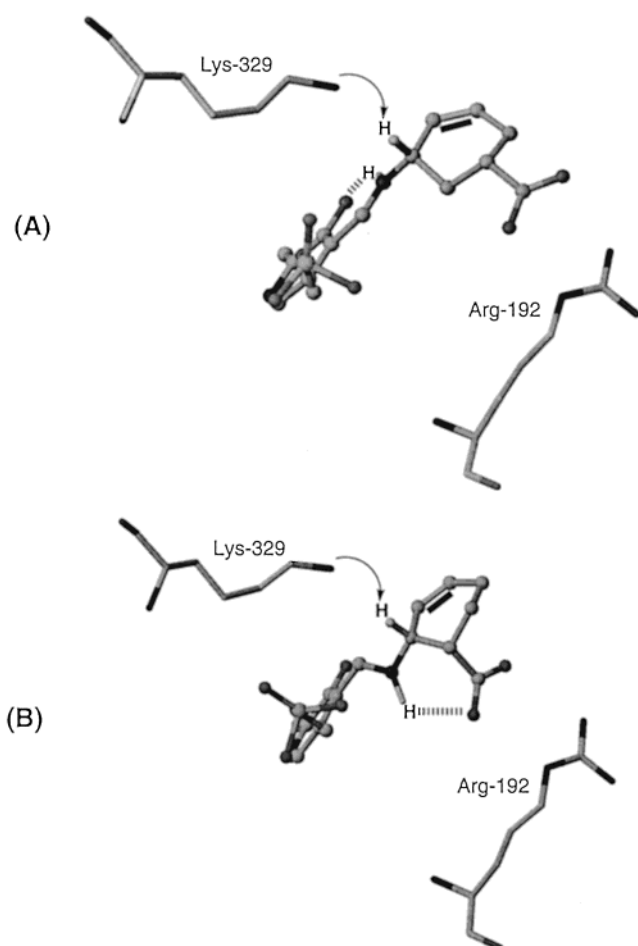


**Figure 6.** Molecular models comparing hydrogen-bonding interactions of **3** and **5**.

structure analysis (Bruker SMART-1000 CCD) and mass spectral analyses (Micromass Quattro II electrospray triple quadrupole) were performed by the Analytical Services Laboratory in the Department of Chemistry, Northwestern University. Electron impact high-resolution mass spectra (HRMS)

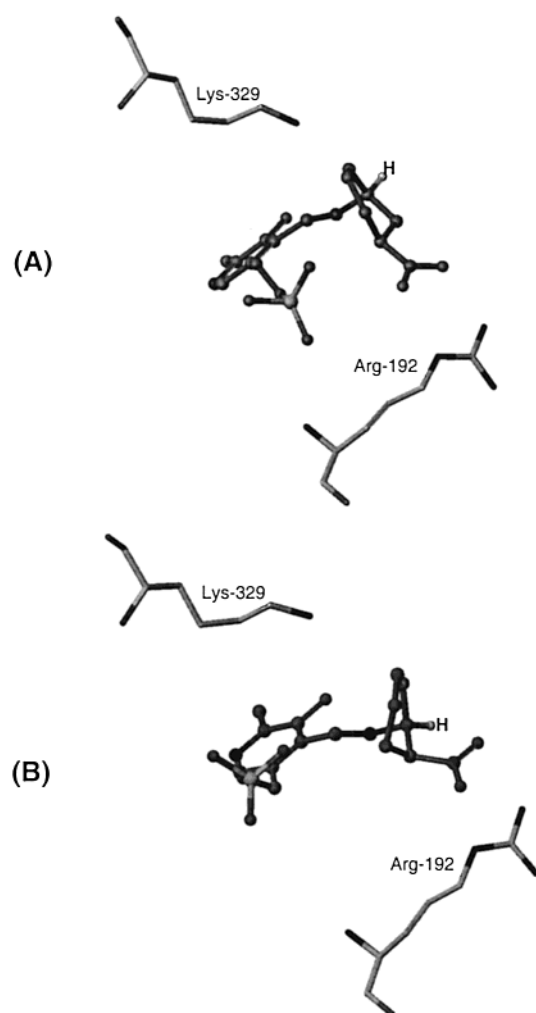


**Figure 7.** Molecular models of **4** and **6**.

were obtained with a VG70-250SE spectrometer. Combustion analyses were performed by Oneida Research Laboratories, NY. Thin-layer chromatography (TLC) was run with silica gel

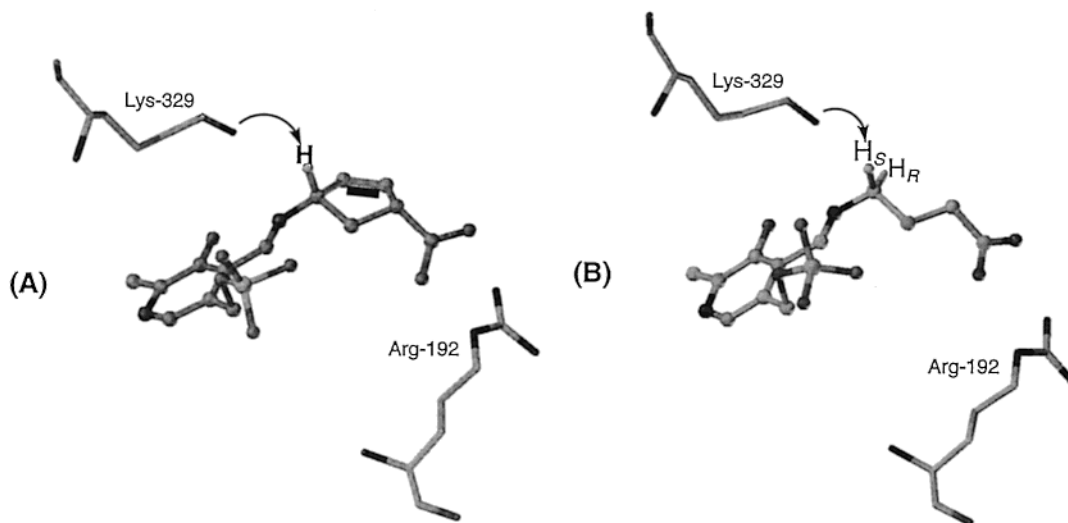
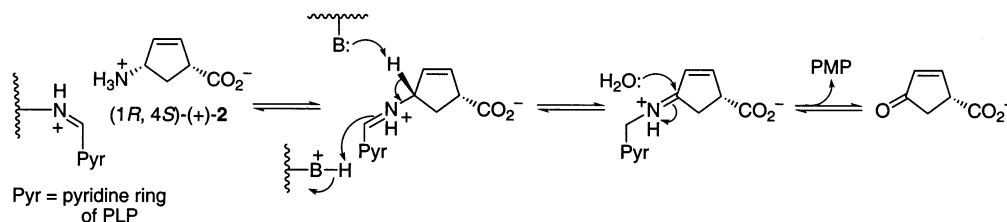


**Figure 8.** Comparison of molecular models of **2** and GABA.

### Scheme 5



60 F<sub>254</sub> precoated glass plates (EM Separations Technology) using standard visualization techniques. Flash column chromatography was carried out with silica gel 60 (230–400 mesh) from Merck. Cation exchange chromatography was performed on Dowex 50 resin (BioRad AG50W-X8, 100–200 mesh, biotech grade). Unless otherwise noted, all reactions were carried out under a nitrogen atmosphere. An Orion research model 701 pH meter with a general combination electrode was used for pH measurements. Enzyme assays were recorded on a Perkin-Elmer Lambda 10 UV/vis spectrophotometer. Radioactivity was measured by liquid scintillation counting using a Packard Tri-Carb 2100TR counter and Packard Ultima Gold scintillation cocktail. HPLC analyses were performed using a Beckman System Gold system with a 125 solvent delivery module and a 166 UV detector.

**Reagents.** All chemicals used in the synthetic procedures were purchased from Aldrich or Fischer Scientific and were used as received unless otherwise noted.  $\alpha$ -Ketoglutarate,  $\beta$ -mercaptoethanol, NADP<sup>+</sup>, Sephadex G50, buffer salts, and other reagents used in the enzymological studies were purchased from Sigma.

**Synthesis of *trans*-3-Aminocyclohex-4-ene-1-carboxylic acid (**4**).** 7-Oxabicyclo[3,2,1]-oct-2-en-6-one (**7**) was synthesized from cyclohex-3-ene-1-carboxylic acid by the procedure of Marshall et al.<sup>17</sup> and was allowed to react with NaN<sub>3</sub> to prepare (*d,l*)-*trans*-3-azidocyclohex-4-ene-1-carboxylic acid (**8**).<sup>16</sup> A mixture of the resulting azide **8** (447 mg, 2.67 mmol) and triphenylphosphine (770 mg, 2.94 mmol) in THF (15 mL) with 1 equiv of water<sup>18</sup> (48  $\mu$ L) was stirred at room temperature for 97 h and then concentrated in vacuo. The residue was partitioned between methylene chloride (15 mL) and 0.5 N HCl (15 mL) in an ice bath. The aqueous phase was further washed with methylene chloride (15 mL  $\times$  3). After the water was removed, the resulting residue was chromatographed on a Dowex 50W (H<sup>+</sup>) cation exchange column by washing the column with water and then eluting with 1 M pyridine. The desired *trans* isomer **4** was recrystallized from ethanol/water (2:1) to give **4** (200 mg, 53%). <sup>1</sup>H NMR (D<sub>2</sub>O):  $\delta$  1.90–2.20 (4H, m, CH<sub>2</sub> and CH<sub>2</sub>), 2.50 (1H, m, CHCO<sub>2</sub>), 3.79 (1H, m, CHN), 5.58 (1H, br d, J 9.9 Hz, =C(4)H), 6.05 (1H, m, 9.9 Hz,

=C(5)H). <sup>13</sup>C NMR (D<sub>2</sub>O):  $\delta$  32.3 (C6), 33.8 (C2), 41.9 (C1), 49.9 (C3), 125.8 (C4), 138.9 (C5), 187.8 (CO<sub>2</sub>). HRMS (EI) (*m/z*): [M – H]<sup>+</sup> calcd for C<sub>7</sub>H<sub>10</sub>NO<sub>2</sub>, 140.0712; found, 140.0718. Anal. calcd for C<sub>7</sub>H<sub>11</sub>NO<sub>2</sub>: C, 59.56; H, 7.85; N, 9.92. Found: C, 59.26; H, 7.97; N, 9.77.

**Synthesis of *cis*- and *trans*-2-Aminocyclohex-3-ene-1-carboxylic Acids (**5** and **6**).** A mixture of ethyl *cis*- and *trans*-6-carbomethoxy-2-cyclohexen-1-yl carbamates (**9** and **10**, in a 4:1 ratio) was prepared from the Diels–Alder reaction of ethyl *trans*-1,3-butadiene-1-carbamate and methyl acrylate<sup>19</sup> and separated by repeated silica gel column chromatography (4:1 hexanes–ethyl acetate; using Silica gel 60 particle size 0.015–0.040 mm from EM Science). To a 2 M solution of the *cis* carbamate **9** (1.125 g, 4.95 mmol) in chloroform, sealed in a reaction vessel under nitrogen, was added 2.5 equiv of iodotrimethylsilane (1.80 mL, 12.4 mmol) via dry syringe. The reaction mixture was then heated at about 55 °C for 12 h. When the reaction was completed (as determined by TLC), 4 equiv of HCl-saturated methanol was added (to quench the reaction so that the amine was protonated as formed).<sup>20</sup> After volatile components were removed under reduced pressure, the *cis* amino acid **5** was purified by a Dowex 50W-X8 cation exchange column (by washing the column with water and then eluting with 1 M pyridine) and then recrystallized from ethanol/water (2:1), yielding 433 mg (62%). In the same manner, the *trans* carbamate **10** (280 mg, 1.23 mmol) was allowed to react with iodotrimethylsilane (440  $\mu$ L, 3.08 mmol) (55 °C for 12 h) and purified to afford the *trans* amino acid **6** (99 mg, 57%). Compound **5**: <sup>1</sup>H NMR (D<sub>2</sub>O):  $\delta$  1.70–2.08 (4H, m, CH<sub>2</sub> and CH<sub>2</sub>), 2.60 (1H, m, CHCO<sub>2</sub>), 3.86 (1H, m, CHN), 5.60 (1H, m, J 10.2 Hz, =C(3)H), 6.0 (1H, m, J 10.2 Hz, =C(4)H). <sup>13</sup>C NMR (D<sub>2</sub>O):  $\delta$  21.8 (C5), 24.1 (C6), 42.2 (C1), 46.8 (C2), 121.8 (C3), 135.0 (C4), 181.0 (CO<sub>2</sub>). HRMS (EI) (*m/z*): [M + H]<sup>+</sup> calcd for C<sub>7</sub>H<sub>12</sub>NO<sub>2</sub>, 142.0868; found, 142.0869. Anal. calcd for C<sub>7</sub>H<sub>11</sub>NO<sub>2</sub>·0.2H<sub>2</sub>O: C, 58.08; H, 7.94; N, 9.68. Found: C, 58.04; H, 8.01; N, 9.65. X-ray crystal structure analysis confirmed the structure, as shown in Figure 1: a colorless square plate crystal of C<sub>7</sub>H<sub>11</sub>NO<sub>2</sub>·C<sub>2</sub>H<sub>5</sub>OH having dimensions of 0.22 mm  $\times$  0.22 mm  $\times$  0.09 mm with *Z* = 4 and the calculated density = 1.24 g/cm<sup>3</sup>. Compound **6**: <sup>1</sup>H NMR

(D<sub>2</sub>O):  $\delta$  1.55–2.05 (4H, m, CH<sub>2</sub> and CH<sub>2</sub>), 2.31 (1H, m, CHCO<sub>2</sub>), 3.92 (1H, m, J 2.20 Hz, CHN), 5.50 (1H, dd, J 2.20, 10.3 Hz, =C(3)H), 5.97 (1H, m, J 10.3 Hz, =C(4)H). HRMS (EI) (*m/z*): [M + H]<sup>+</sup> calcd for C<sub>7</sub>H<sub>12</sub>NO<sub>2</sub>, 142.0868; found, 142.0862. Anal. calcd for C<sub>7</sub>H<sub>11</sub>NO<sub>2</sub>: C, 59.56; H, 7.85; N, 9.92. Found: C, 59.17; H, 7.70; N, 9.87.

**Synthesis of the Expected Product of Enamine Reaction of 5 (11).** PLP (50 mg, 0.2 mmol) and cyclohexanone (23  $\mu$ L, 0.22 mmol) were dissolved in 8 mL of 0.5 M KOH, and the solution was stirred for 24 h in the dark at room temperature. The reaction mixture was adjusted to pH 7.0 with 70% perchloric acid, and the solid KClO<sub>4</sub> was removed after centrifugation. The remaining salt was washed twice with cold water. The combined supernatants were concentrated and applied to a Dowex 50W-X8 cation exchange column. Aliquots of each fraction were spotted on silica gel thin-layer plates, developed in 1-butanol-acetic acid-water (6:2:2 by volume), and characterized with Gibbs reagent.<sup>26</sup> Further purification was carried out with a C<sub>18</sub> reverse-phase HPLC column (with the gradient system of 0.1% trifluoroacetic acid (TFA) in H<sub>2</sub>O and MeOH), and fractions containing the product were collected, concentrated, and lyophilized to give the product **11** (26 mg, 36%). This PLP adduct from the aldol condensation showed a retention time (*T<sub>R</sub>* = 35 min) where multiple products from the incubation mixture of **5** with GABA-AT occur. LC/MS analysis using electrospray ionization showed the protonated molecular ion peak of the product **11**: [M + H]<sup>+</sup> calcd for C<sub>14</sub>H<sub>18</sub>NO<sub>6</sub>P, 327.27; found, 328.0.

**Molecular Modeling.** All procedures were performed using SYBYL molecular modeling software version 6.5 or 6.6 (Tripos, Inc., Saint Louis, MO) operating under IRIX 6.5. The coordinates from the X-ray crystal structure of GABA-AT<sup>22</sup> were used for modeling studies. The docking experiment was performed using the FlexX program<sup>27</sup> interfaced with SYBYL. Water molecules were removed as they were found not to be located within the active site region, and hydrogen atoms on the backbone and side chains were added based on the standard average bond angles and lengths. Dictionary charges from the AMBER force field were added. The active site for docking was defined as all amino acids within 6.5 Å proximity of the cofactor PLP. The investigated ligands were created as external aldimines starting from geometrically optimized fragments. The potential energies were minimized to obtain a comparable starting point for each compound. The Powell conjugate gradient minimizer within the MAXIMIN procedure was used with the parameters of the MMFF94 force field.

For the MD simulation, the docked complex of GABA-AT and *S*-vinyl-GABA was used as the starting structure, and the MMFF94 force field was used. The MD simulation was performed by raising the temperature to 500 K over a period of 5000 fs and cooling to 300 K over a period of 5000 fs with a step size of 1 fs. Trajectories were recorded every 100 fs of simulation and were analyzed.

**Enzymes and Assays.** GABA-AT was isolated from pig brains as described previously.<sup>28</sup> The purified enzyme was approximately 95% homogeneous by sodium dodecyl sulfate polyacrylamide gel electrophoresis (SDS-PAGE) (Coomassie blue). Succinic semialdehyde dehydrogenase (SSDH) was isolated from GABAse (Sigma), and GABA-AT activity was monitored spectrophotometrically via a coupled assay as previously described.<sup>29</sup>

**Time-Dependent Inhibition of GABA-AT.** GABA-AT (15  $\mu$ L, 2.12 mg/mL) was incubated at 25 °C in 150  $\mu$ L total volume of a solution containing various concentrations of **5**, 1 mM  $\alpha$ -ketoglutarate, 5 mM  $\beta$ -mercaptoethanol, and 50 mM potassium pyrophosphate at pH 8.5. An identical sample, which contained no inhibitor, served as the control. At time intervals over 60 min, 10  $\mu$ L aliquots were assayed for enzyme activity.

**Substrate Protection from Inactivation of GABA-AT.** GABA-AT (15  $\mu$ L, 2.12 mg/mL) was incubated at 25 °C in 150  $\mu$ L total volume of a solution containing 10 mM **5**, 5 mM  $\alpha$ -ketoglutarate, 5 mM  $\beta$ -mercaptoethanol, 0–10 mM GABA, and 0.1 M potassium pyrophosphate at pH 8.5. A sample in which the inhibitor was omitted served as the control. At time

intervals over 60 min, 10  $\mu$ L aliquots were removed and assayed for enzyme activity.

**Irreversible Inactivation of GABA-AT.** GABA-AT (15  $\mu$ L, 2.12 mg/mL) was incubated at 25 °C in 150  $\mu$ L total volume of a solution containing 5 mM **5**, 5 mM  $\alpha$ -ketoglutarate, 5 mM  $\beta$ -mercaptoethanol, and 0.1 M potassium pyrophosphate at pH 8.5. Aliquots (10  $\mu$ L) were removed at 0.5 and 17.5 h and assayed for activity. A portion of the incubation mixture (100  $\mu$ L) was applied to a Penefsky spin column<sup>30</sup> prepared with Sephadex G50 in a Bio-Spin disposable chromatography column (BioRad) according to the published procedure. Small molecules were removed by spinning for 2 min on an IEC Clinical centrifuge. A 10  $\mu$ L aliquot was removed and assayed for enzyme activity. An identical sample, which contained no inactivator, served as the control. Experiments were run in duplicate.

**Inactivation of [<sup>3</sup>H]PLP-Reconstituted GABA-AT by 5 and HPLC Analysis.** GABA-AT, which had been reconstituted with [<sup>3</sup>H]PLP as previously described,<sup>31</sup> was incubated at 25 °C and protected from light in 100 mM potassium phosphate containing 112 mM **5**, 5 mM  $\alpha$ -ketoglutarate, and 5 mM  $\beta$ -mercaptoethanol at pH 7.4. A control was run with the same concentrations of each reagent, excluding inactivator, and a second control was run with 40 mM GABA containing no inactivator or  $\alpha$ -ketoglutarate. The first control should release the cofactor as PLP, while the second should release it as PMP. When the enzyme in the inactivator solution was less than 7% active, excess small molecules were removed by running the solutions over Sephadex G-50 using the Penefsky spin method.<sup>30</sup> The pH of each solution was adjusted to 11–12 using 1 M KOH. These were incubated at room temperature for 1 h and added to enough TFA to quench the base and make a 10% v/v TFA solution. After they stood at room temperature for 10 min, the denatured enzyme solutions were placed into prerinsed Centricon 10 microconcentrators and were centrifuged for 20 min at 5000 rpm in a DuPont Sorvall RC5B Plus Centrifuge, using an SA 600 rotor to achieve complete separation of the protein and the effluents. Each Centricon was rinsed with 1 mL of the buffer (containing 100 mM potassium phosphate and 5 mM  $\beta$ -mercaptoethanol at pH 7.4), vortexed, and then centrifuged for an additional 20 min. This was repeated three times, and the rinses were added to the supernatants and then freeze-dried. Analysis of the incubation mixtures was carried out by dissolving the resulting solid in 100  $\mu$ L of water, and then injecting the samples onto an Alltech Econosil C18 reverse-phase HPLC column (4.6 mm  $\times$  250 mm, 10  $\mu$ m). HPLC analysis was done using a mobile phase of H<sub>2</sub>O containing 0.1% TFA flowing at 0.5 mL/min for 15 min. The flow rate was increased to 1.0 mL/min over the next 5 min, and then, a solvent gradient to 100% methanol with 0.1% TFA was run over the next 20 min. The flow rate was further increased to 2.0 mL/min over 5 min and maintained for 15 min, and then, a 10 min solvent gradient to 100% water with 0.1% TFA was run, followed by changing the flow rate to 0.5 mL/min over 5 min. Under these conditions, PLP elutes at 17 min and PMP at 8 min. Fractions were collected every minute, and the elution of radioactivity was followed by liquid scintillation counting. The incubation mixture with fractions, which during previous experiments with [<sup>3</sup>H]PLP-reconstituted GABA-AT with **3** or **5** contained substantial amounts of radioactivity, was analyzed by LC/MS using electrospray (ES<sup>+</sup>) ionization, which confirmed the occurrence of the decarboxylated modified cofactor: [M + H]<sup>+</sup> calcd for C<sub>14</sub>H<sub>18</sub>NO<sub>6</sub>P, 327.27; found, 328.1 for inactivator **5**.

**Competitive Inhibition of GABA-AT.** The activity of GABA-AT upon introduction of varying concentrations (0, 50, 100, 250, 375, 500, 750, and 1000  $\mu$ M) of **4** or **6** was determined spectrophotometrically by measuring the formation of NADH upon the conversion of SSDH at 25 °C and at several GABA concentrations (4, 6, 10, 15, and 25 mM) in 100 mM potassium pyrophosphate buffer at pH 8.5, containing 5 mM  $\beta$ -mercaptoethanol. Kinetic parameters were derived from Dixon<sup>32</sup> and Cornish-Bowden<sup>33</sup> plots with at least five different concentrations of **4** or **6** for every concentration of GABA.



**Acknowledgment.** We thank the National Institutes of Health (Grant NS15703) for financial support of this research.

## References

- (1) (a) Krnjevic, K. Chemical nature of synaptic transmission in vertebrates. *Physiol. Rev.* **1974**, *54*, 418–540. (b) Faingold, C. L.; Gehlbach, G.; Caspary, D. M. On the role of GABA as an inhibitory neurotransmitter in inferior colliculus neurons: iontophoretic studies. *Brain Res.* **1989**, *500*, 302–312. (c) Bohme, I.; Luddens, H. The inhibitory neural circuitry as target of antiepileptic drugs. *Curr. Med. Chem.* **2001**, *8*, 1257–1274.
- (2) Cooper, A. J. L. Glutamate- $\gamma$ -aminobutyrate transaminase. *Methods Enzymol.* **1985**, *113*, 80–82.
- (3) Gale, K. GABA in epilepsy: the pharmacologic basis. *Epilepsia* **1989**, *30* (Suppl. 3), S1–S11.
- (4) (a) Hornykiewicz, O.; Lloyd, K. G.; Davidson, L. The GABA system, function of the basal ganglia and Parkinson's disease. In *GABA in Nervous System Function*; Roberts, E., Chase, T. N., Tower, D. B., Eds.; Raven Press: New York, 1976; pp 479–485. (b) Kleppner, S. R.; Tobin, A. J. GABA signaling: Therapeutic targets for epilepsy, Parkinson's disease and Huntington's disease. *Emerging Ther. Targets* **2001**, *5*, 219–239.
- (5) Perry, T. L.; Hansen, S.; Kloster, M. Huntington's chorea: deficiency of  $\gamma$ -aminobutyric acid in brain. *N. Engl. J. Med.* **1973**, *288*, 337–342.
- (6) (a) Aoyagi, T.; Wada, T.; Nagai, M.; Kojima, F.; Harada, S.; Takeuchi, T.; Takahashi, H.; Hirokawa, K.; Tsumita, T. Increased  $\gamma$ -aminobutyrate aminotransferase activity in brain of patients with Alzheimer's disease. *Chem. Pharm. Bull.* **1990**, *38*, 1748–1749. (b) Weiner, M. F. Treatment of behavioral/psychological symptoms in Alzheimer's disease. *Exp. Rev. Neurother.* **2001**, *1*, 70–80.
- (7) (a) Kushner, S. A.; Dewey, S. L.; Kornetsky, C. The irreversible  $\gamma$ -aminobutyric acid (GABA) transaminase inhibitor  $\gamma$ -vinyl-GABA blocks cocaine self-administration in rats. *J. Pharmacol. Exp. Ther.* **1999**, *290*, 797–802. (b) Dewey, S. L.; Morgan, A. E.; Ashby, C. R., Jr.; Horan, B.; Kushner, S. A.; Logan, J.; Volkow, N. D.; Fowler, J. S.; Gardner, E. L.; Brodie, J. D. A novel strategy for the treatment of cocaine addiction. *Synapse* **1998**, *30*, 119–129.
- (8) Lippert, B.; Metcalf, B. W.; Jung, M. J.; Casara, P. 4-Amino-hex-5-enoic Acid, a Selective Catalytic Inhibitor of 4-Aminobutyric-Acid Aminotransferase in Mammalian Brain. *Eur. J. Biochem.* **1977**, *74*, 441–445.
- (9) Nanavati, S. M.; Silverman, R. B. Design of Potential Anticonvulsant Agents: Mechanistic Classification of GABA Aminotransferase Inactivators. *J. Med. Chem.* **1989**, *32*, 2413–2421.
- (10) (a) Silverman, R. B. *Mechanism-Based Enzyme Inactivation: Chemistry and Enzymology*; CRC Press: Boca Raton, 1988; Vols. I and II. (b) Silverman, R. B. Mechanism-Based Enzyme Inactivators. *Methods Enzymol.* **1995**, *249*, 240–283.
- (11) Davies, J. A. Mechanism of action of antiepileptic drugs. *Seizure* **1995**, *4*, 267–271.
- (12) Brennan, M. Treating substance abuse. *Chem. Eng. News* **1999**, August 23, 8.
- (13) Nanavati, S. M.; Silverman, R. B. Mechanism of Inactivation of  $\gamma$ -Aminobutyric Acid Aminotransferase by the Antiepilepsy Drug  $\gamma$ -Vinyl GABA (Vigabatrin). *J. Am. Chem. Soc.* **1991**, *113*, 9341–9349.
- (14) Choi, S.; Storici, P.; Schirmer, T.; Silverman, R. B. Design of a Conformationally Restricted Analogue of the Antiepilepsy Drug Vigabatrin that Directs Its Mechanism of Inactivation of  $\gamma$ -Aminobutyric Acid Aminotransferase. *J. Am. Chem. Soc.* **2002**, *124*, 1620–1624.
- (15) Qiu, J.; Pingsterhaus, J. M.; Silverman, R. B. Inhibition and Substrate Activity of Conformationally Rigid Vigabatrin Analogues with  $\gamma$ -Aminobutyric Acid Aminotransferase. *J. Med. Chem.* **1999**, *42*, 4725–4728.
- (16) Murahashi, S.-I.; Taniguchi, Y.; Imada, Y.; Tanigawa, Y. Palladium(0)-Catalyzed Azidation of Allyl Esters. Selective Synthesis of Allyl Azides, Primary Allylamines, and Related Compounds. *J. Org. Chem.* **1989**, *54*, 3292–3303.
- (17) Marshall, J. A.; Xie, S. Synthesis of a C22-34 Subunit of the Immunosuppressant FK-506. *J. Org. Chem.* **1995**, *60*, 7230–7237.
- (18) Nagarajan, S.; Ganem, B. Chemistry of Naturally Occurring Polyamines. 11. Unsaturated Spermidine and Spermine Derivatives. *J. Org. Chem.* **1987**, *52*, 5044–5046.
- (19) Overman, L. E.; Taylor, G. F.; Houk, K. N.; Domelsmith, L. N. Diels–Alder Reactions between *trans*-1-N-Acylamino-1,3-dienes and Methyl Acrylate. A Correlation between Diene Photoelectron Ionization Potentials and Reactivity, Stereoselectivity, and Regioselectivity. *J. Am. Chem. Soc.* **1978**, *100*, 3182–3189.
- (20) (a) Jung, M. E.; Lyster, M. A. Conversion of Alkyl Carbamates into Amines via Treatment with Trimethylsilyl Iodide. *J. Chem. Soc. Chem. Commun.* **1978**, 315–316. (b) Jung, M. E.; Lyster, M. A. Quantitative Dealkylation of Alkyl Esters via Treatment with Trimethylsilyl Iodide. A New Method for Ester Hydrolysis. *J. Am. Chem. Soc.* **1977**, *99*, 968–969.
- (21) Kitz, R.; Wilson, I. B. Esters of Methanesulfonic Acid as Irreversible Inhibitors of Acetylcholinesterase. *J. Biol. Chem.* **1962**, *237*, 3245–3249.
- (22) Storici, P.; Capitani, G.; De Biase, D.; Moser, M.; John, R. A.; Jansonius, J. N.; Schirmer, T. Crystal Structure of GABA-aminotransferase, a Target for Antiepileptic Drug Therapy. *Biochemistry* **1999**, *38*, 8628–8634.
- (23) (a) De Biase, D.; Barra, D.; Bossa, F.; Pucci, P.; John, R. A. Chemistry of the Inactivation of 4-Aminobutyrate Aminotransferase by the Antiepileptic Drug Vigabatrin. *J. Biol. Chem.* **1991**, *266*, 20056–20061. (b) De Biase, D.; Bolton, J. B.; Barra, D.; Bossa, F.; John, R. A. Stoichiometry and stability of the adduct formed between human 4-aminobutyrate aminotransferase and 4-amino-hex-5-enoate: sequence of a labelled peptide. *Biochimie* **1989**, *71*, 491–495.
- (24) Toney, M. D.; Pascarella, S.; De Biase, D. Active Site Model for  $\gamma$ -Aminobutyrate Aminotransferase Explains Substrate Specificity and Inhibitor Reactivities. *Protein Sci.* **1995**, *4*, 2366–2374.
- (25) Dunathan, H. C. Conformation and Reaction Specificity in Pyridoxal Phosphate Enzymes. *Proc. Natl. Acad. Sci. U.S.A.* **1966**, *55*, 712–716.
- (26) Ross, J. H. 2,6-Dichloroquinone 4-Chloroimide as a Reagent for Amines and Aromatic Hydrocarbons on Thin-layer Chromatograms. *Anal. Chem.* **1968**, *40*, 2138–2143.
- (27) Rarey, M.; Kramer, B.; Lengauer, T.; Klebe, G. A Fast Flexible Docking Method Using an Incremental Construction Algorithm. *J. Mol. Biol.* **1996**, *261*, 470–489.
- (28) Johnson, T. R.; Silverman, R. B. Syntheses of (*Z*)- and (*E*)-4-Amino-2-(trifluoromethyl)-2-butenic Acid and Their Inactivation of  $\gamma$ -Aminobutyric Acid Aminotransferase. *Bioorg. Med. Chem.* **1999**, *7*, 1625–1636.
- (29) Silverman, R. B.; Bichler, K. A.; Leon, A. J. Mechanisms of inactivation of  $\gamma$ -aminobutyric acid aminotransferase by 4-amino-5-fluoro-5-hexenoic acid. *J. Am. Chem. Soc.* **1996**, *118*, 1241–1252.
- (30) Penefsky, H. S. A centrifuged-column procedure for the measurement of ligand binding by beef heart F1. *Methods Enzymol.* **1979**, *56*, 527.
- (31) Fu, M.; Silverman, R. B. Isolation and characterization of the product of inactivation of  $\gamma$ -aminobutyric acid aminotransferase by gabaculine. *Bioorg. Med. Chem.* **1999**, *7*, 1581–1590.
- (32) Dixon, M. The Determination of Enzyme Inhibitor Constants. *Biochem. J.* **1953**, *55*, 170–171.
- (33) Cornish-Bowden, A. *Fundamentals of Enzyme Kinetics*; Portland Press: London, 1995; pp 102–108.

JM020134I